Improving Uplink Scalability of LoRa-Based Direct-to-Satellite IoT Networks

Sergio Herrería-Alonso, *Senior Member, IEEE*, Miguel Rodríguez-Pérez, *Senior Member, IEEE*, Raúl F. Rodríguez-Rubio, and Fernando Pérez-Fontán

Abstract—In the next few years, low-Earth orbit (LEO) constellations will become key enablers for the deployment of global Internet of Things (IoT) services. Due to their proximity to Earth, LEO satellites can directly communicate with ground nodes and, thus, serve as mobile gateways for IoT devices deployed in remote areas lacking terrestrial infrastructure. Within this Direct-to-Satellite IoT (DtS-IoT) context, LoRa technology, capable of providing long-range connectivity to power-constrained devices, has received great attention. However, serious scalability issues have been observed in LoRa-based DtS-IoT networks when a high number of LoRa devices perform uplink transmissions driven by the straightforward Aloha protocol during the short visibility periods of the passing-by satellites. In this article, we evaluate some Aloha-based protocols suitable for this kind of networks and present a new adaptive variant that allows LoRa devices to dynamically adjust their uplink transmission rates in order to make the network work near its optimal operating point. Simulation results show that our proposal is able to significantly improve the network throughput in overloaded scenarios without the need for coordination among LoRa devices, listening to the channel nor gateway support.

Index Terms—Aloha, Direct-to-Satellite Internet of Things (DtS-IoT), long range (LoRa), LoRaWAN, low-Earth orbit (LEO), medium access control (MAC).

I. INTRODUCTION

INTERNET of Things (IoT) technologies have been gaining increasing attention during the last years [1]. In this context, one of the most ambitious technological challenges is the deployment of global IoT-based services [2]. Certainly, many different applications, such as fleet management, transportation, environment monitoring, or emergency management, could benefit from the operation of global IoT networks covering remote areas that, either for technical or economic reasons, lack terrestrial connectivity.

Satellite networks are a promising solution to provide global IoT services in a flexible and affordable way [3], [4], [5]. The idea consists on connecting IoT devices placed in areas without terrestrial infrastructure directly to a constellation of satellites passing over them. In this Direct-to-Satellite IoT

(DtS-IoT) paradigm [6], [7], satellites act as gateways that collect the messages from the IoT devices and store them for a short period until they eventually forward the messages downlink when passing over a gateway on the surface.

Low-Earth orbit (LEO) constellations are ideal candidates for implementing DtS-IoT networks [8], [9], [10]. Thanks to their low altitude orbits (160–1000 km), LEO constellations can provide global coverage with lower deployment costs, link budgets, and propagation delays than other constellations at higher altitudes. However, due to their low altitude, LEO satellites orbit at high speeds (about 8 km/s). This causes some significant impairments on the satellite links related to the Doppler effect and also reduces the visibility time over a particular region to just a few minutes. In any case, these issues have not prevented a number of companies, such as Iridium [11], Globalstar [12], Astrocast [13], and Lacuna Space [14], from successfully providing global DtS-IoT connectivity using their own LEO constellations.

At the same time, recent studies have shown the enormous potential of low-power wide-area networks (LPWANs) technologies, such as NB-IoT [15], Sigfox [16], or LoRaWAN [17], as low-cost solutions for achieving DtS-IoT connectivity [4], [9], [18]. Clearly, using current LPWAN standards in the Earth-to-satellite link favors seamless interoperability of LEO constellations with existing ground IoT infrastructure. Moreover, LPWAN technologies are able to provide long-range (LoRa) connectivity with low energy consumption, so, despite their low transmission rates, they emerge as very attractive solutions for DtS-IoT networks in which power-constrained IoT devices just send some short messages occasionally.

LoRaWAN is an open protocol designed and maintained by the LoRa Alliance that enables devices to communicate using LoRa wireless technology [17]. Within main LPWAN technologies, LoRaWAN is the one with the lowest power requirements and costs [19], [20], so we focus in this article on LoRa-based DtS-IoT networks in which IoT devices use LoRaWAN for communicating directly with LEO satellites. The feasibility of LoRa-based DtS-IoT networks is well established and some companies like Lacuna Space [14] and Wyld [21] already enable direct connection of LoRa devices with their own LEO constellations. However, a critical issue related to their scalability has been identified [22], [23], [24]. The coverage area of LEO satellites will potentially include a high number of devices that will attempt an uplink transmission during the limited visibility periods in which the gateways

installed on the satellites are available. Since LoRa devices follow a simple Aloha-based protocol for accessing the channel, they will transmit their messages without restraint, thus causing large amounts of collisions. LoRa-based DtS-IoT networks require, therefore, more sophisticated medium access control (MAC) schemes to cope with these dense scenarios and improve scalability [25], [26].

In this article, we first evaluate some random access MAC protocols that could be suitable for LoRa-based DtS-IoT networks. Due to the severely limited processing, communication, and power capacities of commonly deployed LoRa devices, we restrict the proposed schemes to variants of the straightforward Aloha protocol. Our experiments confirm that, as expected, the throughput that can be obtained with these simple MAC protocols is quite limited and, what is worse, rapidly degrades as the traffic load increases.

To improve uplink scalability in overloaded scenarios, we propose a novel Aloha variant that allows LoRa devices to dynamically adjust their transmission rates so that the network always works near its optimal operating conditions. Performance results show that our transmission control mechanism is able to substantially increase the throughput obtained in these DtS-IoT networks when the number of connected devices is high. Moreover, the proposed scheme can be easily implemented even in the most simple LoRa devices since each node can autonomously adjust its sending rate without the need for coordination among active nodes, listening to the channel nor gateway support.

The remainder of this article is organized as follows. Related work is reviewed in Section II. Section III describes in detail the DtS-IoT network model assumed in this article. In Section IV, we present different Aloha-based MAC strategies suitable for LoRa-based DtS-IoT networks. Among them, we present a new adaptive Aloha variant that allows LoRa devices to dynamically adjust their transmission rates in order to make the network work around its optimum operation point. Performance results are shown in Section V. Finally, Section VI summarizes the main conclusions of this work.

II. RELATED WORK

In this section, we briefly describe the main LoRa and LoRaWAN features, and review the latest MAC schemes proposed for LoRa-based DtS-IoT networks.

A. LoRa/LoRaWAN

LoRaWAN is an open communication protocol built upon the proprietary LoRa transmission technology developed by Semtech [17]. LoRa defines a physical layer based on a sub-GHz spread spectrum modulation technique optimized for long-range, low-power transmissions [27]. Several LoRa radio parameters can be configured: the spreading factor (SF), ranging from 7 to 12, to tradeoff between the bit rate, the coverage range, and the energy consumption[1]; the *channel bandwidth* (BW), from 7.8 to 500 kHz, to balance between

the reception sensitivity and the bit rate; and the coding rate (CR), to specify the number of overhead symbols added to protect the LoRa signal against interference.

Although LoRa technology was not expressly designed for DtS-IoT networks, it can be successfully applied to them [28], [29]. Recently, Semtech has proposed LoRa frequency-hopping spread spectrum (LR-FHSS), an extension of the LoRa physical layer that is more suitable for these highly long-range and large-scale communication scenarios [30]. However, LR-FHSS is still not very widespread, so we will assume in this article that IoT devices use the legacy LoRa physical layer.

In a LoRaWAN network, end devices (EDs) can only communicate with a gateway (GW). The GW operates as a relay, that is, it receives LoRa messages from EDs and simply forwards them to the network server that manages the LoRaWAN network. LoRaWAN specifies three modes of operation for the EDs (classes A, B, and C). Class A EDs use a simple Aloha-based protocol to transmit to the GW, so they just send their messages without using any control mechanism, thus causing a large amount of collisions when the network load is high. Each uplink transmission is then followed by one or two short downlink receiving windows that allow the GW to send acknowledgments or commands to the EDs. In contrast, Class B EDs repeatedly open downlink receiving windows according to a network-defined schedule. For this, the GW periodically sends beacons to synchronize the EDs and inform them of the next downlink slots. Finally, Class C EDs continuously listen for downlink messages except when they are transmitting. Note that Class B and Class C devices do not need a previous uplink communication for receiving a downlink message. In this work, we focus on Class A EDs because they are the least energy demanding ones, and this is the only mode common to all LoRa devices.

B. MAC Schemes for LoRa-Based DtS-IoT Networks

There are plenty of works proposing enhanced MAC protocols to improve the scalability of terrestrial LoRaWAN networks [31], [32], [33]. Unfortunately, they cannot be directly applied to DtS-IoT scenarios due to the specific features of the satellite link (i.e, limited availability, long distances, large delays, and strong fluctuations).

Most of the works evaluating LoRa-based DtS-IoT networks assume that EDs transmit using either the standard Aloha-based protocol [28], [34], [35], [36] or the slotted Aloha (S-Aloha) variant that splits the channel into discrete timeslots and forces EDs to init their transmissions at the beginning of a timeslot [37].

In recent years, new MAC protocols have been specifically proposed for LoRa-based DtS-IoT scenarios. For example, [23] presents SALSA, a scheduling algorithm for uplink transmissions that minimizes the occurrence of collisions. However, the deployment of scheduled time-slotted MAC mechanisms in LoRaWAN networks is really complicated since these schemes require an accurate synchronization mechanism [38] and scheduling a variable number of ED transmissions with limited downlink availability [32].

---

[1]The SF controls how much a symbol is spread over time. Thus, higher SFs allow covering wider areas at the cost of decreasing the bit rate and drawing more energy.

To control the number of contending devices, [24] proposes that the GW at the satellite informs the EDs of the expected number of them that want to transmit during the next frame. Then, with this information, each ED will determine the transmission probability in the current frame using a so-called skip function. In a similar way, [39] proposes that the GW uses an estimator of the number of competing nodes to compute the probability of collision in a given frame. Then, the GW broadcasts this probability to the EDs so that they decide whether to transmit in the current frame. In RESS-IoT [40], the GW broadcasts a beacon frame to announce its presence to the EDs. After receiving the beacon, each ED with pending data to transmit attempts to reserve a timeslot sending a request-to-send (RTS) frame to the GW. Then, the GW assigns different timeslots to those EDs that succeeded in transmitting their RTS frames and informs them sending a clear-to-send (CTS) frame. However, note that all these approaches require the transmission of periodic beacons in the downlink, so they are suitable for Class B or Class C EDs, but not for the Class A ones.

There also exist multiple schemes that combine packet replication and interference cancellation techniques to improve the throughput of satellite networks [22], [41], [42]. However, these time diversity techniques not only increase complexity and power consumption at the EDs but also impose stringent requirements in terms of memory and computational load to the GW. This renders them inappropriate for LEO satellites with limited computational resources.

Finally, carrier sensing protocols (CSMA and its variants) are also unsuitable for DtS-IoT scenarios since, in these networks, the probability of hidden nodes is too high and the propagation delays are too large [25], [43].

In short, DtS-IoT networks for LoRaWAN Class A nodes require energy efficient MAC protocols that can be deployed on resource-constrained devices with limited processing and communication capacities. In this article, we will explore some random access MAC protocols that could be adopted for these scenarios.

III. DtS-IoT Network Model

We consider a LoRa-based DtS-IoT network in which a number of EDs located on the ground try to directly send their messages through LoRa links to a GW located on a LEO satellite. The satellite passes from time to time over a circular region in which the EDs are uniformly distributed, so each ED will perceive a slightly different and dynamic uplink channel. To avoid wasting energy in useless transmissions, we assume that the EDs are configured with some kind of information about the satellite trajectory (during the activation phase, for example) and that, therefore, they are aware of the visibility periods of the satellite (i.e., the availability times of the GW).

We only consider uplink traffic from the EDs to the GW. Also, we assume that only one uplink transmission is allowed per ED within a single visibility period. This is the most likely scenario due to the short visibility periods of LEO satellites and LoRa duty cycle restrictions.

A. Propagation Channel

Our scenario fulfills line-of-sight conditions since the direct signals from the EDs will be received at the satellite with much more power than their possible multipath echoes. We assume however that the link is affected by multipath given the nondirective characteristics of the LoRa antennas. Therefore, we can model the uplink channel with a Rice distribution [44] and the power of the signal received at the satellite (in dBm) can be computed as

$$P_{rx} = P_{tx} + G_{tx} + G_{rx} + L_{fs} + L_{rice} - L_{sys} \qquad (1)$$

where P_{tx} is the ED transmission power (in dBm), G_{tx} and G_{rx} are, respectively, the transmitter and the receiver antenna gains when compared to an isotropic antenna with unit gain (in dBi), L_{fs} is the propagation path loss in free space (in dB), L_{rice} is the Rician fading (in dB), and L_{sys} are miscellaneous system losses due to, for example, polarization mismatches or atmospheric events (in dB).

Using the Friis formula, the propagation path loss is given by

$$L_{fs} = 20 \log_{10} \left(\frac{\lambda}{4\pi d} \right) \qquad (2)$$

where λ is the carrier wavelength, and d is the distance between the ED and the satellite (both in meters). Note that this term has to be summed to the transmitted power since $d \gg \lambda$ (far field condition) and, therefore, it is already negative.

Finally, the Rician fading can be computed as

$$L_{rice} = 20 \log_{10} \left(\sqrt{(1 + s_1 \sigma)^2 + (s_2 \sigma)^2} \right) \qquad (3)$$

where s_1 and s_2 are two normalized Gaussian random samples, and $\sigma = 1/\sqrt{2 \cdot 10^{k/10}}$. Here, k is the ratio between the power of the direct signal and the power of the multipath component (in dB). Finally, if the satellite elevation angle α is known (in degrees), [45] shows that it is possible to estimate the k factor using the following empirically derived expression:

$$k = 2.731 - 0.1074 \alpha + 0.002774 \alpha^2. \qquad (4)$$

B. Capture Effect

Considering that LoRa SFs are quasi-orthogonal [46] and multiple orthogonal transmission channels are provided for each BW, it can be assumed that a collision will only take place when two or more EDs send their messages on the same SF and channel at the same time. To guarantee that all uplink transmissions reach the GW with sufficient power, we consider that all the EDs transmit to the satellite using SF12, the most robust one, although at the cost of higher consumptions and longer transmission times. Therefore, overlapping ED transmissions on the same uplink channel will cause the collision of the corresponding LoRa signals.

Nonetheless, thanks to the capture effect observed on LoRa signals [47], the receiver at the satellite could successfully demodulate the strongest signal out of those that have collided

provided that its signal-to-interference ratio (SIR) is higher than a given threshold γ, that is, if

$$\text{SIR} = \frac{P_{\text{rx}}^j}{\sum_{i=1, i \neq j}^n P_{\text{rx}}^i} \geq \gamma \qquad (5)$$

where P_{rx}^i, $i = 1, \ldots, n$, is the power of each of the n interfering signals, and P_{rx}^j is the power of the strongest signal among the n interfering ones.

IV. MAC SCHEMES

Class A EDs currently use a straightforward Aloha-based protocol: they just send a frame when they have some data to send. However, as previously explained, we will assume that EDs know the future visibility periods of the satellites so that they can save energy by simply postponing their transmissions (temporarily storing their data) until a satellite is in sight again. For this scenario, we propose different variants of the Aloha protocol that cope with the demands of Class A EDs in terms of energy efficiency and complexity. Note that all of them could benefit from the capture effect of LoRa signals just additionally applying interference cancellation at the receiver.

A. Classical Aloha Schemes

Certainly, Class A EDs could apply typical Aloha and S-Aloha MAC protocols, but only during the periods in which they have a satellite in sight.

1) Aloha: Unfortunately, using Aloha directly in this scenario would cause a large number of collisions. Note that, with this scheme, all EDs with pending data to send will initiate their transmissions as soon as their respective visibility periods begin and, therefore, the transmissions of those EDs in close proximity to each other would collide permanently.

2) Slotted Aloha: In this scheme, the uplink channel is divided into discrete timeslots of equal length so that EDs are forced to start their transmissions at the beginning of a timeslot. Even though slotted schemes are known to reduce the number of collisions, there will still be many collisions in this scenario since all EDs would schedule their transmissions at the first timeslot in the next visibility period. In addition, slotted schemes require a synchronization mechanism to define the timeslots. Although the synchronization details are beyond the scope of our paper, there exist several lightweight synchronization mechanisms that could be used in this scenario [38], [48], [49].

B. Random Aloha Schemes

To reduce collisions at the beginning of visibility periods, we propose to randomize the times when EDs start their transmissions.

1) Random Aloha (R-Aloha): With this scheme, if an ED has some data pending to send, it will randomly choose the starting time of the consequent transmission within the next visibility period.

2) Random Slotted Aloha: Similarly, with random S-Aloha (RS-Aloha), each ED will randomly select a timeslot in the next visibility period and then start transmitting the frame at the beginning of the selected timeslot.

C. Adaptive Random Aloha Schemes

It is widely known that, for any multiple access channel, the network throughput increases with the offered load until it reaches a certain value. From that point on, increasing the offered load just worsens the system performance since the amount of collisions rises dramatically and, therefore, the throughput decreases. In this section, we propose a novel adaptive mechanism so that the EDs can adjust their transmission rates and keep the network close to its optimal operation point in a dynamic and autonomous manner.

1) Adaptive Random Aloha (AR-Aloha): Let G be the normalized offered load, that is, the average number of EDs attempting a transmission per frame transmission time, and S be the normalized throughput, that is, the average number of successful transmissions per frame transmission time. It is well known that, if the number of EDs attempting to transmit follows a Poisson distribution and all frames require the same transmission time, the normalized throughput for an Aloha system can be calculated as $S = Ge^{-2G}$. This expression is also asymptotically true with a large number of dissimilar EDs, each one having an arbitrary distribution of frame interarrival times, as in our scenario [50]. At the same time, if p_{success} is the probability of success for the transmission of a frame, it also holds that $S = p_{\text{success}}G$. So, equating both expressions and solving for G, we get that the EDs can easily estimate the normalized offered load as

$$\hat{G} = -\frac{\log(\hat{p}_{\text{success}})}{2} \qquad (6)$$

if they are able to obtain an estimation $\hat{p}_{\text{success}}$ of the probability of transmission success.

Another well-known result for Aloha systems is that the normalized throughput is maximum when $G^* = 0.5$. Thus, to maximize the amount of successful transmissions, the load offered to the network should be maintained around this optimum G^* value. For this, we propose that each ED autonomously decides whether to transmit in the visibility period i on the basis of a given transmission probability $p_{\text{tx}}[i]$ tuned in accordance with the current system load. For instance, if the offered load estimated at the visibility period i, $\hat{G}[i]$, is greater than G^*, it can be considered that the system is overloaded and, therefore, the network load should be reduced by decreasing $p_{\text{tx}}[i]$. Conversely, if $\hat{G}[i] < G^*$, the offered load is low enough and $p_{\text{tx}}[i]$ can be increased.

We propose to update the transmission probability every visibility period using a conventional closed-loop controller with error signal $G^* - \hat{G}[i]$ as shown in Fig. 1. The controller operations are described in detail in Algorithm 1. The proportionality constant is set to $\kappa/\hat{G}[i]$ to obtain a good tradeoff between p_{tx} stability and an agile response to varying traffic conditions. Also note that, to avoid the starvation of the EDs, we do not allow p_{tx} to take a value lower than p_{min}. The stability of this dynamic algorithm is evaluated in the Appendix.

2) Adaptive Random Slotted Aloha (ARS-Aloha): Evidently, the proposed algorithm can also be applied to S-Aloha systems but, in these scenarios, the normalized throughput must be computed as $S = Ge^{-G}$. So, equating
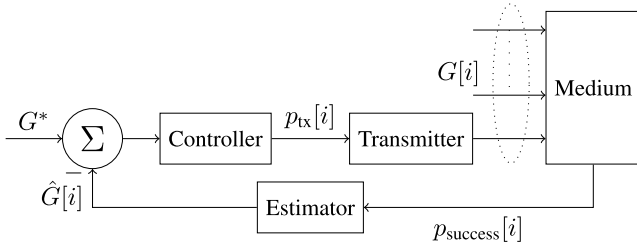
Fig. 1. Block diagram of the proposed closed-loop load controller. The actual load offered to the system can be regulated by adjusting the transmission probability of each active ED. This probability is updated each visibility period so that the system load tends to the optimal value. Each ED can autonomously estimate the offered load from the transmission success probability it observes.

Algorithm 1 Tuning Algorithm of p_{tx} Executed at Each ED Every Visibility Period i

---

Require: Estimation of the probability of success of a frame transmission ($\hat{p}_{success}[i]$). Initially, $p_{tx}[0] \leftarrow 1$.

  if slotted **then**

    /* Adaptive Random Slotted Aloha (ARS-Aloha) */

    $\hat{G}[i] = -\log(\hat{p}_{success}[i])$

    $G^* = 1$

  else

    /* Adaptive Random Aloha (AR-Aloha) */

    $\hat{G}[i] = -\log(\hat{p}_{success}[i])/2$

    $G^* = 0.5$

  end if

  $p_{tx}[i] \leftarrow p_{tx}[i-1] + \dfrac{\kappa}{\hat{G}[i]}\left(G^* - \hat{G}[i]\right)$

  if $p_{tx}[i] > 1$ **then**

    $p_{tx}[i] \leftarrow 1$

  else if $p_{tx}[i] < p_{min}$ **then**

    $p_{tx}[i] \leftarrow p_{min}$

  end if

---

this to $p_{success}G$ and solving for G, we now get that the EDs should estimate the offered load as

$$\hat{G} = -\log(\hat{p}_{success}). \tag{7}$$

On the other hand, the maximum throughput in slotted systems is obtained when $G^* = 1$. Algorithm 1 shows the tuning procedure of p_{tx} for both slotted and unslotted variants.

3) Estimation of Transmission Success Probability: As just explained, in order to estimate the offered load at any given time, each ED must obtain an accurate estimation of the probability of success of a frame transmission by its own. Note that all EDs will obtain a sample $p_{success}[i]$ of this probability each time they send a frame: $p_{success}[i] = 1$ if the frame is successfully transmitted in the visibility period i, $p_{success}[i] = 0$ otherwise. We propose that each ED then estimates the success probability as an exponentially weighted moving average (EWMA) of the obtained samples

$$\hat{p}_{success}[i+1] = \beta p_{success}[i] + (1-\beta)\hat{p}_{success}[i], \ 0 < \beta < 1 \tag{8}$$

to assign more weight to newer samples and, thus, react quicker to load changes. And in the case that an ED does not eventually send a frame in the visibility period i, its
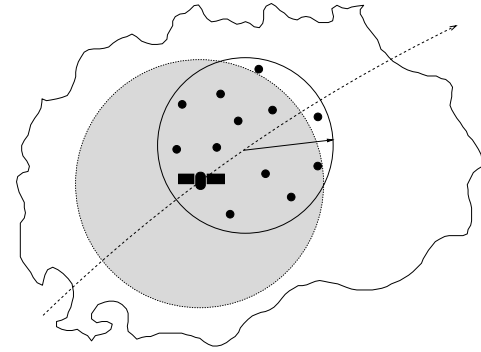

Fig. 2. Simulated scenario. EDs are uniformly distributed in a circular area with a radius of 100 km, so they perceive slightly different uplink channels. The satellite footprint is shown as a gray circle.

estimation of the success probability will remain unchanged: $\hat{p}_{success}[i+1] = \hat{p}_{success}[i]$. This EWMA estimator will eventually converge to the actual average value as long as the number of active EDs (regardless of whether they eventually transmit or not according to their transmission probability) remains stable.

V. EXPERIMENTAL RESULTS

To compare the performance of the considered MAC protocols, we have conducted several simulation experiments using a LEO constellation simulator module [51] we developed for the ndnSIM network simulator [52]. In particular, we have simulated a DtS-IoT scenario with a single LEO satellite configured with an orbit at an altitude of 500 km and an inclination angle of 60°. As shown in Fig. 2, the EDs are uniformly distributed at random locations in a circular region of 100-km radius around a given central point over which the satellite passes from time to time. Consequently, the EDs observe slightly different not totally overlapped visibility periods. We assume that the uplink is operative when the elevation angle is higher than 25°. We have simulated multiple visibility periods of significant duration. In particular, the duration of the visibility periods in the simulated scenarios varies from 201 to 230 s (with average ≈ 216 s).

We have configured LoRa parameters with the default values for the EU868 band, as shown in Table I. We assumed that all LoRa frames carry the same payload (20 bytes), thus requiring each one a transmission time (time on air) of 1.319 s with SF12 [53]. Therefore, the average number of EDs that could successfully transmit a frame per visibility period is upper bounded to $\lfloor 216/1.319 \rfloor = 163$.

Table II shows the values assigned to the main power parameters. Note that we assumed the maximum allowed transmission power for the EDs (14 dBm), 0-dBi gain antennas at 868 MHz on the EDs, a 12-dBi gain antenna on the satellite, and system losses of 3.3 dB due to polarization mismatches and atmospheric issues as suggested in [29]. We have checked that, with this power configuration, almost all uplink transmissions are received at the satellite with a power higher than the reception sensitivity threshold for SF12 (−137 dBm). Finally, when interference cancellation is applied at the receiver, we set the capture effect threshold γ to 1 dB, as in [54] and [55].
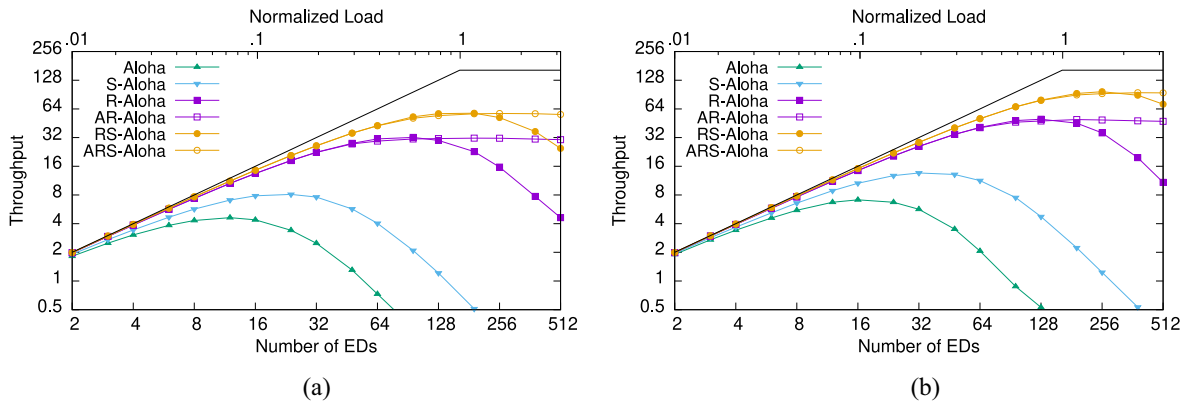
Fig. 3.   Throughput results. (a) Without interference cancellation. (b) With interference cancellation.

TABLE I
LoRa CONFIGURATION PARAMETERS

Parameter	Value
SF	12
BW	125 kHz
CR	4/5
Frequency	868 MHz
Symbol duration	32.77 ms
Preamble length	8 symbols
Payload length	20 bytes
Time on air	1.319 s
Data rate	0.293 kb/s

TABLE II
POWER PARAMETERS

Parameter	Value
P_{tx}	14 dBm
G_{tx}	0 dBi
G_{rx}	12 dBi
L_{sys}	3.3 dB
γ	1 dB

Regarding the slotted schemes, we set the timeslot duration to 1.451 s, that is, the frame transmission time plus a 10% guard time to deal with slight de-synchronizations. Finally, for the adaptive schemes, the smoothing factor β, the closed-loop proportionality constant κ and the minimum transmission probability p_{min} are set to 1/8, 1/4, and 1/8, respectively. With these values of p_{min} and κ, the system stability conditions derived in the Appendix are met for all the simulated scenarios.

A. Throughput

We first examined the available throughput varying the number of active EDs on the uplink channel from 2 to 512 (i.e., varying the normalized offered load from 0.012 to 3.13). Fig. 3 shows the throughput obtained with the different MAC schemes measured as the average number of EDs that are able to successfully transmit a frame per visibility period. The maximum throughput achievable with an ideal MAC scheme is also shown with a black line as a reference.

Certainly, the throughput obtained with all the Aloha-based schemes is modest: on average, the slotted (unslotted) variants can achieve a maximum of just 58 (32) successful

transmissions per visibility period. And, as expected, the throughput obtained with the classical variants is very poor since they cause a large number of collisions at the beginning of the visibility periods.[2] Also note that, for the randomized variants, the throughput decreases as the offered load exceeds the optimum value (i.e., a normalized load of 0.5 for the unslotted schemes and 1 for the slotted ones). However, with our adaptive transmission control, the throughput at the highest loads can be maintained at the maximum value, without compromising network performance at low and moderate loads. As expected, the EDs are able to dynamically adjust their transmission rates so that the effective offered load tends to the optimum value. It is worth noting that, although our model implicitly assumes that the EDs observe completely overlapped visibility periods, it is also valid when the EDs observed only partially overlapped visibility periods of similar duration, as is the case in the simulated scenarios.

Fig. 4 shows how the transmission probability (the average value of p_{tx} for all active EDs) evolves in both unslotted and slotted scenarios. It can be seen how the EDs opportunely respond to traffic overload by reducing their transmission probabilities proportionally to the actual excess load. In addition, as predicted by the stability analysis, the transmission probability converges after a moderate number of visibility periods in all the simulated scenarios.[3] For this, both p_{min} and κ parameters have been configured with values that satisfy their respective stability conditions derived in the Appendix: $p_{min} = 1/8 < p_{tx}^* < 0.19$ (the lowest p_{tx}^* value obtained with 512 EDs in the unslotted scenario) and $0 < \kappa = 1/4 < 2G^*/G < 0.32$ (the lowest threshold obtained when $G^* = 0.5$ and $G = 3.13$). Finally, note that if the number of active EDs (i.e., the offered load) is low enough, the EDs always keep their transmission

[2]This is the expected performance in single satellite scenarios with very sparse visibility periods. As the number of satellites in the LEO constellation increases, the visibility periods will become more frequent and the throughput obtained with the classical variants will approach that of the randomized ones.

[3]The actual convergence time depends on the frequency of the visibility periods. In this scenario with a single LEO satellite at an altitude of 500 km, EDs just enjoy a visibility period approximately every 90 min, so the proposed algorithm would take about 60 h to converge. However, LEO constellations actually consist of multiple satellites distributed among a set of different orbital planes, so the times between successive visibility periods are significantly shorter and, therefore, our algorithm will take much less time to converge.
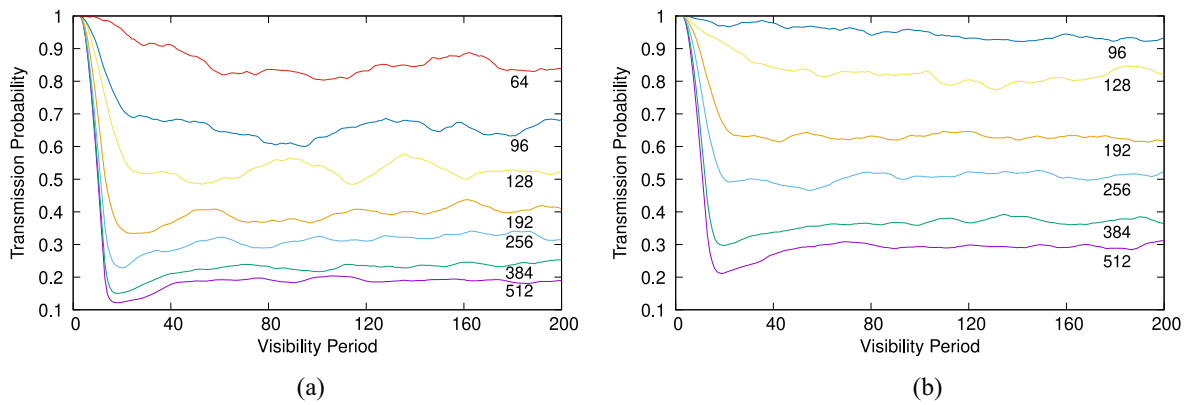
Fig. 4. Evolution of the average transmission probability at the EDs. Each line is labeled with the corresponding number of active EDs. (a) Unslotted scenarios. (b) Slotted scenarios.
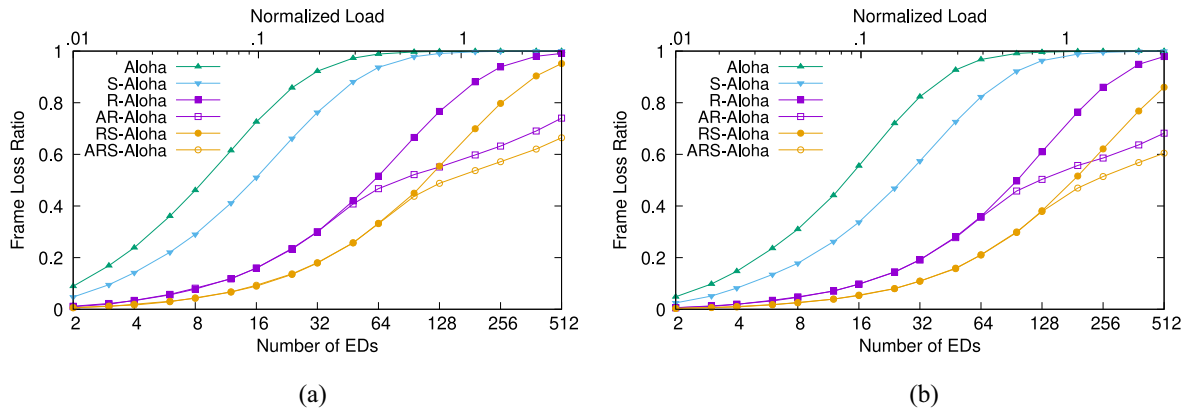

Fig. 5. FLR results. (a) Without interference cancellation. (b) With interference cancellation.

probabilities very close to 1 and, therefore, it is unnecessary to show the results for these scenarios in the graphs.

Fig. 3(b) depicts the throughput obtained when interference cancellation is applied at the GW. The results are analogous to those obtained without interference cancellation although, in these scenarios, the average number of successful transmissions per visibility period is higher (at most 97 and 50 for the slotted and the unslotted schemes, respectively). Note that our adaptive techniques still work well even with interference cancellation and keep the throughput at its maximum value at the highest loads.

B. Frame Loss Ratio

The frame loss ratio (FLR) is another metric commonly used to evaluate the performance of MAC mechanisms. FLR is defined as the ratio of failing transmissions (i.e., FLR= $1 - p_{\text{success}}$). Fig. 5 shows the FLR obtained with the different schemes in the previous scenarios. It can be seen that the FLR increases quickly with the number of active EDs although, as expected, lower FLRs are measured when using the slotted schemes. Additionally, note that the adaptive variants can partially mitigate the FLR increment at the highest loads since they significantly reduce the effective load offered to the network.

Alternately, MAC performance can be evaluated by estimating the offered load that can be supported while keeping the FLR around a target value. Thus, we show in Fig. 6
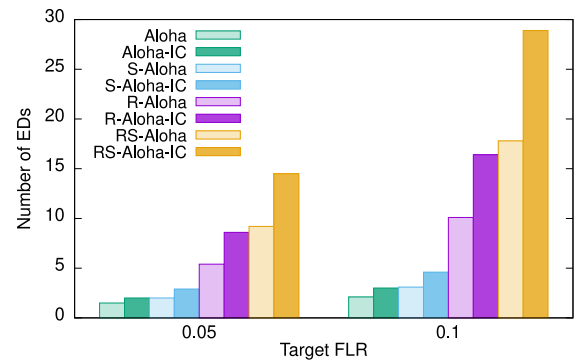

Fig. 6. Target FLR results.

the number of active EDs supported with each scheme when considering target FLRs of just 0.05 and 0.1. Certainly, to maintain the FLR at such low values, the number of active EDs must be necessarily small, especially without interference cancellation. Note that the values obtained with the adaptive schemes are not depicted in this graph since they are identical to those obtained with their corresponding unresponsive schemes (as expected, both adaptive and nonadaptive schemes provide equal FLRs at low loads).

C. Energy Efficiency

We have also evaluated the efficiency of the MAC schemes at the EDs from an energy point of view. The energy efficiency can be defined as the average number of bits that EDs can
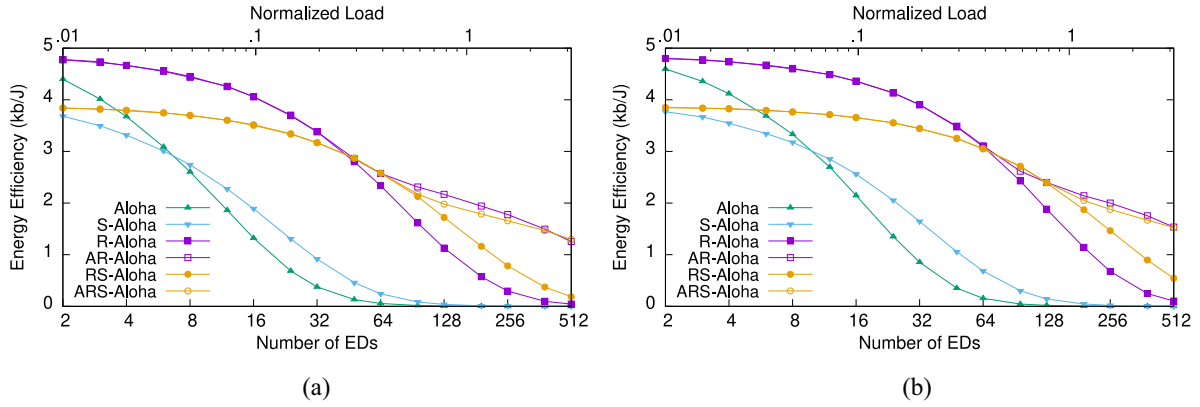
Fig. 7. Energy efficiency results. (a) Without interference cancellation. (b) With interference cancellation.

successfully transmit through the uplink channel per joule

$$\text{Energy efficiency} = (1 - \text{FLR}) \frac{N}{P_{\text{tx}} T + E_{\text{sync}}} \qquad (9)$$

where N is the average number of bits in the payload of the successfully transmitted frames, T is the average frame transmission time, and E_{sync} is the energy consumed by the synchronization mechanism necessary in the slotted schemes. In our experiments, recall that we set $P_{\text{tx}} = 14\,\text{dBm} = 25.12\,\text{mW}$ and, since we assumed that all LoRa frames carry 20 bytes in their payload, we get that $N = 160\,\text{bits}$ and $T = 1.319\,\text{s}$. Certainly, slotted schemes require consuming some additional energy E_{sync} to maintain EDs synchronized. Fortunately, lightweight synchronization mechanisms just require the occasional reception of beacon frames from the GW at long intervals. Thus, if we assume that at most one beacon frame must be received every two visibility periods, we get that $E_{\text{sync}} = P_{\text{sync}} T_{\text{beacon}}/2$, where P_{sync} is the power consumed by an ED while sensing the downlink channel and T_{beacon} is the transmission time of the beacon frames.

Fig. 7 shows the energy efficiency obtained for the MAC schemes assuming that $P_{\text{sync}} = P_{\text{tx}}/2 = 12.56\,\text{mW}$ and that the beacons have the same length that the data frames ($T_{\text{beacon}} = T = 1.319\,\text{s}$). Clearly, energy efficiency decreases as the offered load increases since, as shown in (9), it is inversely proportional to the FLR. Also note that, at low loads, the unslotted schemes are more efficient than the slotted ones since the marginally lower FLRs obtained with the slotted schemes do not compensate for the energy consumed by the synchronization mechanism. However, in overloaded scenarios, the situation is just reversed and the slotted schemes become more efficient. Another important result is that the adaptive schemes significantly improve energy efficiency at the highest loads since they greatly reduce the amount of failing transmissions. Finally, note that MAC schemes with interference cancellation are, of course, slightly more efficient: the application of interference cancellation techniques reduces the FLR at the cost of increasing the energy consumption at the GW, but it has no power effect on the EDs at all.

VI. Conclusion

This article addresses the scalability issues raised on DtS-IoT networks in which LoRa devices use LoRaWAN technology for communicating directly with LEO satellites. It is expected that coverage areas of LEO satellites will include a high number of devices attempting an uplink transmission during the short visibility periods of the passing-by gateways. Therefore, the conventional Aloha protocol used by LoRa devices may be unsuitable for these scenarios.

In this article, we have evaluated some different Aloha-based MAC schemes that can cope with the stringent demands of resource-constrained LoRa devices in terms of energy efficiency and complexity. Simulation results show that the throughput obtained with all the evaluated schemes is modest and that, therefore, the number of active EDs in these networks should be limited in some way. Additionally, we have presented a novel technique that allows LoRa devices to dynamically adapt their sending rates so that the network always works near its optimal operating conditions. As a result, our adaptive Aloha variants, unlike common Aloha-based schemes, are able to obtain a throughput near the maximum achievable even in overloaded scenarios. Moreover, the proposed technique can be easily implemented in any kind of LoRa device, since each node can autonomously adjust its sending rate without the need for coordination among active nodes, listening to the channel nor gateway support.

Appendix
Stability Analysis

The adaptive p_{tx} tuning algorithm presented in Algorithm 1 can be modeled as the following dynamical system:

$$p_{\text{tx}}[i] = \min\left\{\max\left\{p_{\text{tx}}[i-1] + \frac{\kappa}{\hat{G}[i]}\left(G^* - \hat{G}[i]\right), p_{\min}\right\}, 1\right\} \qquad (10)$$

in the discrete index $i = 1, 2, \ldots$, where $\hat{G}[i] = p_{\text{tx}}[i-1]\, G$ captures the impact of the transmission probability on the effective offered load. Since $\hat{G}(\cdot)$ is a continuous, increasing and differentiable function of p_{tx} with bounded derivative, this system clearly reaches the equilibrium point p_{tx}^* when $\hat{G}(p_{\text{tx}}^*) = p_{\text{tx}}^* G = G^*$. Then, assuming $p_{\min} \leq p_{\text{tx}}^* \leq 1$ since,

otherwise, the target load G^* cannot be achievable, (10) can be written as

$$p_{\text{tx}}[i] = p_{\text{tx}}[i-1] + \kappa \left(\frac{G^*}{p_{\text{tx}}[i-1]G} - 1 \right).$$ (11)

It is straightforward to prove via linearization that this system is stable if the derivative of (11) at the equilibrium point has an absolute value strictly less than one, that is

$$\left| 1 - \kappa \frac{G^*}{G p_{\text{tx}}^{*2}} \right| < 1.$$ (12)

Therefore, the stability condition is met if $0 < \kappa < 2Gp_{\text{tx}}^{*2}/G^*$. Finally, substituting $p_{\text{tx}}^* = G^*/G$ in this expression, we get that $0 < \kappa < 2G^*/G$ to guarantee system stability. Clearly, both G^* and G are bounded and positive, so there always exists a sufficiently small κ that holds with the required stability condition.

REFERENCES

[1] M. Chui, M. Collins, and M. Patel, *IoT Value Set to Accelerate Through 2030: Where and How to Capture It*. New York, NY, USA: McKinsey & Company, 2021. [Online]. Available: https://www.mckinsey.com/capabilities/mckinsey-digital/our-insights/iot-value-set-to-accelerate-through-2030-where-and-how-to-capture-it

[2] M. R. Palattella and N. Accettura, "Enabling Internet of everything everywhere: LPWAN with satellite backhaul," in *Proc. Glob. Inf. Infrastruct. Netw. Symp. (GIIS)*, Thessaloniki, Greece, Oct. 2018, pp. 1–5.

[3] M. De Sanctis, E. Cianca, G. Araniti, I. Bisio, and R. Prasad, "Satellite communications supporting Internet of Remote Things," *IEEE Internet Things J.*, vol. 3, no. 1, pp. 113–123, Feb. 2016.

[4] M. Centenaro, C. E. Costa, F. Granelli, C. Sacchi, and L. Vangelista, "A survey on technologies, standards and open challenges in satellite IoT," *IEEE Commun. Surveys Tuts.*, vol. 23, no. 3, pp. 1693–1720, 3rd Quart., 2021.

[5] M. Koziol. "Satellites can be a surprisingly great option for IoT, IEEE Spectrum." 2021. [Online]. Available: https://spectrum.ieee.org/satellites-great-option-iot

[6] J. A. Fraire, S. Céspedes, and N. Accettura, "Direct-to-satellite IoT–A survey of the state of the art and future research perspectives," in *Ad-Hoc, Mobile, and Wireless Networks*. Cham, Switzerland: Springer, Sep. 2019, pp. 241–258.

[7] J. A. Fraire, O. Iova, and F. Valois, "Space-terrestrial integrated Internet of Things: Challenges and opportunities," *IEEE Commun. Mag.*, vol. 60, no. 12, pp. 64–70, Dec. 2022.

[8] Z. Qu, G. Zhang, H. Cao, and J. Xie, "LEO satellite constellation for Internet of Things," *IEEE Access*, vol. 5, pp. 18391–18401, 2017.

[9] I. F. Akyildiz and A. Kak, "The Internet of Space Things/CubeSats," *IEEE Netw.*, vol. 33, no. 5, pp. 212–218, Sep./Oct. 2019.

[10] M. Feldmann, J. A. Fraire, F. Walter, and S. C. Burleigh, "Ring road networks: Access for anyone," *IEEE Commun. Mag.*, vol. 60, no. 4, pp. 38–44, Apr. 2022.

[11] "Iridium." Accessed: Oct. 11, 2023. [Online]. Available: https://www.iridium.com/network/

[12] (Globalstar, Covington, LA, USA). Accessed: Oct. 11, 2023. [Online]. Available: https://www.globalstar.com/en-us/about/our-technology

[13] "Astrocast-taking IoT further." Accessed: Oct. 11, 2023. [Online]. Available: https://www.astrocast.com/technology/

[14] (Lacuna space, Fremont, CA, USA). Accessed: Oct. 11, 2023. [Online]. Available: https://lacuna.space/about/

[15] Y.-P. E. Wang et al., "A primer on 3GPP narrowband Internet of Things," *IEEE Commun. Mag.*, vol. 55, no. 3, pp. 117–123, Mar. 2017.

[16] (Sigfox, Labège, France). Accessed: Oct. 11, 2023. [Online]. Available: https://www.sigfox.com/

[17] (LoRa Alliance, Fremont, CA, USA). "LoRaWAN specification v1.1." Accessed: Oct. 11, 2023. [Online]. Available: https://lora-alliance.org/resource_hub/lorawan-specification-v1--1/

[18] G. M. Capez, S. Henn, J. A. Fraire, and R. Garello, "Sparse satellite constellation design for global and regional direct-to-satellite IoT services," *IEEE Trans. Aerosp. Electron. Syst.*, vol. 58, no. 5, pp. 3786–3801, Oct. 2022.

[19] K. Mekki, E. Bajic, F. Chaxel, and F. Meyer, "A comparative study of LPWAN technologies for large-scale IoT deployment," *ICT Exp.*, vol. 5, no. 1, pp. 1–7, Mar. 2019.

[20] R. Marini, K. Mikhaylov, G. Pasolini, and C. Buratti, "Low-power wide-area networks: Comparison of LoRaWAN and NB-IoT performance," *IEEE Internet Things J.*, vol. 9, no. 21, pp. 21051–21063, Nov. 2022.

[21] "Wyld networks." Accessed: Oct. 11, 2023. [Online]. Available: https://wyldnetworks.com/

[22] B. Zhao, G. Ren, X. Dong, and H. Zhang, "Optimal irregular repetition slotted ALOHA under total transmit power constraint in IoT-oriented satellite networks," *IEEE Internet Things J.*, vol. 7, no. 10, pp. 10465–10474, Oct. 2020.

[23] M. Afhamisis and M. R. Palattella, "SALSA: A scheduling algorithm for LoRa to LEO satellites," *IEEE Access*, vol. 10, pp. 11608–11615, 2022.

[24] G. Álvarez, J. A. Fraire, K. A. Hassan, S. Céspedes, and D. Pesch, "Uplink transmission policies for LoRa-based direct-to-satellite IoT," *IEEE Access*, vol. 10, pp. 72687–72701, 2022.

[25] T. Ferrer, S. Céspedes, and A. Becerra, "Review and evaluation of MAC protocols for satellite IoT systems using nanosatellites," *Sensors*, vol. 19, no. 8, p. 1947, Apr. 2019.

[26] W. Xiao, M. Kaneko, N. El Rachkidy, and A. Guitton, "Integrating LoRa collision decoding and MAC protocols for enabling IoT massive connectivity," *IEEE Internet Things Mag.*, vol. 5, no. 3, pp. 166–173, Sep. 2022.

[27] T. Elshabrawy and J. Robert, "Interleaved chirp spreading LoRa-based modulation," *IEEE Internet Things J.*, vol. 6, no. 2, pp. 3855–3863, Apr. 2019.

[28] T. Wu, D. Qu, and G. Zhang, "Research on LoRa adaptability in the LEO satellites Internet of Things," in *Proc. 15th Int. Wireless Commun. Mobile Comput. Conf. (IWCMC)*, Tangier, Morocco, Jun. 2019, pp. 131–135.

[29] G. Colavolpe, T. Foggi, M. Ricciulli, Y. Zanettini, and J.-P. Mediano-Alameda, "Reception of LoRa signals from LEO satellites," *IEEE Trans. Aerosp. Electron. Syst.*, vol. 55, no. 6, pp. 3587–3602, Dec. 2019.

[30] G. Boquet, P. Tuset-Peiró, F. Adelantado, T. Watteyne, and X. Vilajosana, "LR-FHSS: Overview and performance analysis," *IEEE Commun. Mag.*, vol. 59, no. 3, pp. 30–36, Mar. 2021.

[31] L. Beltramelli, A. Mahmood, P. Österberg, and M. Gidlund, "LoRa beyond ALOHA: An investigation of alternative random access protocols," *IEEE Trans. Ind. Informat.*, vol. 17, no. 5, pp. 3544–3554, May 2021.

[32] D. Zorbas and X. Fafoutis, "Time-slotted LoRa networks: Design considerations, implementations, and perspectives," *IEEE Internet Things Mag.*, vol. 4, no. 1, pp. 84–89, Mar. 2021.

[33] P. Gkotsiopoulos, D. Zorbas, and C. Douligeris, "Performance determinants in LoRa networks: A literature review," *IEEE Commun. Surveys Tuts.*, vol. 23, no. 3, pp. 1721–1758, 3rd Quart., 2021.

[34] T. Deng, J. Zhu, and Z. Nie, "An adaptive MAC protocol for SDCS system based on LoRa technology," in *Proc. 2nd Int. Conf. Autom. Mech. Control Comput. Eng. (AMCCE)*, Beijing, China, Mar. 2017, pp. 825–830.

[35] M. A. Ullah, K. Mikhaylov, and H. Alves, "Enabling mMTC in remote areas: LoRaWAN and LEO satellite integration for offshore wind farm monitoring," *IEEE Trans. Ind. Informat.*, vol. 18, no. 6, pp. 3744–3753, Jun. 2022.

[36] M. A. Ullah, A. Yastrebova, K. Mikhaylov, M. Höyhtyä, and H. Alves, "Situational awareness for autonomous ships in the arctic: MMTC direct-to-satellite connectivity," *IEEE Commun. Mag.*, vol. 60, no. 6, pp. 32–38, Jun. 2022.

[37] F. A. Tondo, S. Montejo-Sánchez, M. E. Pellenz, S. Céspedes, and R. D. Souza, "Direct-to-satellite IoT slotted aloha systems with multiple satellites and unequal erasure probabilities," *Sensors*, vol. 21, p. 7099, Oct. 2021.

[38] C. Garrido-Hidalgo et al., "LoRaWAN scheduling: From concept to implementation," *IEEE Internet Things J.*, vol. 8, no. 16, pp. 12919–12933, Aug. 2021.

[39] K. Vogelgesang, J. A. Fraire, and H. Hermanns, "Uplink transmission probability functions for LoRa-based direct-to-satellite IoT: A case study," in *Proc. IEEE Glob. Commun. Conf. (GLOBECOM)*, Madrid, Spain, Dec. 2021, pp. 1–6.

[40] R. Ortigueira, J. A. Fraire, A. Becerra, T. Ferrer, and S. Céspedes, "RESS-IoT: A scalable energy-efficient MAC protocol for direct-to-satellite IoT," *IEEE Access*, vol. 9, pp. 164440–164453, 2021.

[41] G. Liva, "Graph-based analysis and optimization of contention resolution diversity slotted ALOHA," *IEEE Trans. Commun.*, vol. 59, no. 2, pp. 477–487, Feb. 2011.
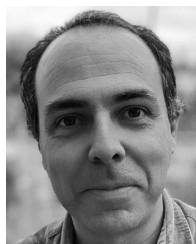
[42] X. Shao, Z. Sun, M. Yang, S. Gu, and Q. Guo, "NOMA-based irregular repetition slotted ALOHA for satellite networks," *IEEE Commun. Lett.*, vol. 23, no. 4, pp. 624–627, Apr. 2019.

[43] S. Herrería-Alonso, A. Suárez-González, M. Rodríguez-Pérez, and C. López-García, "Enhancing LoRaWAN scalability with longest first slotted CSMA," *Comput. Netw.*, vol. 216, Oct. 2022, Art. no. 109252.

[44] F. Pérez Fontán and P. Mariño Espiñeira, *Modeling the Wireless Propagation Channel*. Hoboken, NJ, USA: Wiley, 2008.

[45] G. Corazza and F. Vatalaro, "A statistical model for land mobile satellite channels and its application to nongeostationary orbit systems," *IEEE Trans. Veh. Technol.*, vol. 43, no. 3, pp. 738–742, Aug. 1994.

[46] F. Benkhelifa, Y. Bouazizi, and J. A. McCann, "How orthogonal is LoRa modulation?" *IEEE Internet Things J.*, vol. 9, no. 20, pp. 19928–19944, Oct. 2022.

[47] J. M. de Souza Sant'Ana, A. Hoeller, R. D. Souza, H. Alves, and S. Montejo-Sánchez, "LoRa performance analysis with superposed signal decoding," *IEEE Wireless Commun. Lett.*, vol. 9, no. 11, pp. 1865–1868, Nov. 2020.

[48] M. Rizzi, A. Depari, P. Ferrari, A. Flammini, S. Rinaldi, and E. Sisinni, "Synchronization uncertainty versus power efficiency in LoRaWAN networks," *IEEE Trans. Instrum. Meas.*, vol. 68, no. 4, pp. 1101–1111, Apr. 2019.

[49] T. Polonelli, D. Brunelli, A. Marzocchi, and L. Benini, "Slotted aloha on LoRaWAN-design, analysis, and deployment," *Sensors*, vol. 19, no. 4, p. 838, Feb. 2019.

[50] D. Sant, "Throughput of unslotted ALOHA channels with arbitray packet interarrival time distributions," *IEEE Trans. Commun.*, vol. 28, no. 8, pp. 1422–1425, Aug. 1980.

[51] M. Rodríguez-Pérez and S. Herrería-Alonso. *A LEO Constellation Simulator Module for NdnSIM*. Universidade de Vigo, Vigo, Spain, 2022. [Online]. Available: https://github.com/ICARUS-ICN/icarus-ndnsim

[52] "ndnSIM: NS-3 based NDN simulator." Accessed: Oct. 11, 2023. [Online]. Available: https://github.com/named-data-ndnSIM/ndnSIM

[53] "LoRaTools." Accessed: Oct. 11, 2023. [Online]. Available: https://loratools.nl/#/airtime

[54] D. Croce, M. Gucciardo, S. Mangione, G. Santaromita, and I. Tinnirello, "LoRa technology demystified: From link behavior to cell-level performance," *IEEE Trans. Wireless Commun.*, vol. 19, no. 2, pp. 822–834, Feb. 2020.

[55] W. Zhou, T. Hong, X. Ding, and G. Zhang, "LoRa performance analysis for LEO satellite IoT networks," in *Proc. 13th Int. Conf. Wireless Commun. Signal Process. (WCSP)*, Changsha, China, Oct. 2021, pp. 1–5.

Miguel Rodríguez-Pérez (Senior Member, IEEE) was born in Vigo, Spain, in 1978. He received the M.Sc. and Ph.D. degrees in telecommunication engineering from the University of Vigo, Vigo, in 2001 and 2006, respectively.

He is currently an Associate Professor with the Department of Telematics Engineering, Universidade de Vigo, where he is also an Affiliated Member of the co-located Networking Laboratory. He has coauthored more than 60 conference and journal papers. His research interests, ranging from performance evaluation and congestion control protocols to energy efficiency, are primarily focused on computer networks. In recent years, he has focused on exploring how satellite networks can benefit from new network architectures.

Raúl F. Rodríguez-Rubio received the M.Sc. and Ph.D. degrees in telecommunication engineering from the University of Vigo, Vigo, Spain, in 1991 and 2000, respectively.

He is currently an Associate Professor with the Department of Telematics Engineering, University of Vigo, where he is also an Affiliated Member of the co-located Networking Laboratory. His research interests include quality of service in Internet, performance analysis of computer networks, energy efficiency in communication networks, and new protocols and architectures for the future Internet.

Sergio Herrería-Alonso (Senior Member, IEEE) received the M.Sc. and Ph.D. degrees in telecommunication engineering from the University of Vigo, Vigo, Spain, in 2001 and 2006, respectively.

Since 2010, he has been an Associate Professor with the Department of Telematics Engineering, University of Vigo, where he is also an Affiliated Member of the co-located Networking Laboratory. He has coauthored more than 50 papers in peer-reviewed international conferences and journals, most of them with a high-impact factor (Q1 and Q2 quartiles) in the WOS Journal Citation Report. His main research interests include energy-efficient networking, IoT technologies and networks, and satellite communications.

Fernando Pérez-Fontán was born in Villagarcía de Arosa, Spain. He received the M.Sc. and Ph.D. degrees in telecommunication engineering from the Technical University of Madrid, Madrid, Spain, in 1982 and 1992, respectively.

He is currently a Full Professor with the Telecommunication Engineering School, University of Vigo, Vigo, Spain, where he is also with the atlanTTic Research Center. He has authored a number of international journal articles and conference papers. He has coauthored the book *Modeling the Wireless Propagation Channel: A Simulation Approach With MATLAB* (Wiley, 2008). His current research interests include terrestrial and satellite mobile communications, and fixed radio communication propagation channel modeling.